OPEN

Experimental & Molecular Medicine (2018) 50, e438; doi:10.1038/emm.2017.254
Official journal of the Korean Society for Biochemistry and Molecular Biology
www.nature.com/emm

ORIGINAL ARTICLE

Arginase II inhibition prevents interleukin-8 production through regulation of p38 MAPK phosphorylation activated by loss of mitochondrial membrane potential in nLDL-stimulated hAoSMCs

Bon-Hyeock Koo[1,7], Bong-Gu Yi[1,7], Myeong-Seon Jeong[2], Seung-Hea Kwon[2], Kwang-Lae Hoe[3], Young-Guen Kwon[4], Moo-Ho Won[5], Young-Myeong Kim[6] and Sungwoo Ryoo[1]

Arginase inhibition exhibits beneficial effects in vascular endothelial and smooth muscle cells. In human aortic smooth muscle cells (hAoSMCs), native low-density lipoprotein (nLDL) induced the production of interleukin-8 (IL-8) that is involved in the pathogenesis of cardiovascular diseases. Therefore, we examined the effect of arginase inhibition on IL-8 production and the underlying mechanism. In hAoSMCs, reverse transcription–PCR, western blotting and immunocytochemistry with MitoTracker confirmed that arginase II was confined predominantly to mitochondria. The mitochondrial membrane potential (MMP) was assessed using tetramethylrhodamine ethyl ester. The MMP decreased upon nLDL stimulation but was restored upon arginase inhibition. MMP loss caused by nLDL was prevented by treatment with the intracellular Ca^{2+} chelator BAPTA-AM. In mitochondrial Ca^{2+} measurements using Rhod-2 AM, increased mitochondrial Ca^{2+} levels by nLDL were inhibited upon preincubation with an arginase inhibitor. Among the polyamines, spermine, an arginase activity-dependent product, caused mitochondrial Ca^{2+} movement. The nLDL-induced MMP change resulted in p38 mitogen-activated protein kinase (MAPK) phosphorylation and IL-8 production and was prevented by the arginase inhibitors BAPTA and ruthenium 360. In isolated AoSMCs from $ApoE^{-/-}$ mice fed a high-cholesterol diet, arginase activity, p38 MAPK phosphorylation, spermine and mitochondrial Ca^{2+} levels and keratinocyte-derived chemokine (KC) production were increased compared with wild-type (WT) mice. However, in AoSMCs isolated from arginase II-null mice, increases in MMP and decreases in mitochondrial Ca^{2+} levels were noted compared with WT and were associated with p38 MAPK activation and IL-8 production. These data suggest that arginase activity regulates the change in MMP through Ca^{2+} uptake that is essential for p38 MAPK phosphorylation and IL-8 production.

Experimental & Molecular Medicine (2018) **50,** e438; doi:10.1038/emm.2017.254; published online 2 February 2018

INTRODUCTION

Atherosclerosis is considered a chronic inflammatory disease initiated by diverse stimuli. Among a variety of stimuli, lipid accumulation is by far the most favorably substantiated factor in atherosclerosis. Extracellular lipid accumulation occurs early in the response to elevated plasma levels of native low-density lipoprotein (nLDL), and nLDL exerts negative effects on vascular homeostasis, such as induction of proliferation and vasoconstriction of human aortic smooth muscle cells (hAoSMCs).[1,2] We demonstrated that stimulation of hAoSMCs by nLDL induced interleukin-8 (IL-8) production and major signaling events, resulting in H_2O_2 generation and p38 mitogen-activated protein kinase (MAPK) activation.[3] Thus, IL-8 exerted an autocrine effect that evoked the migration of hAoSMCs.[4] The mouse chemokine KC is an analog of IL-8 and a member of the CXC chemokine family. KC is upregulated and participates in neutrophil activation and monocyte migration to the subendothelial space in the early phase of atherosclerosis.[5]

Two isoforms of arginase, arginase I and II, are encoded by distinct genes. These isoforms exhibit different tissue

[1]Department of Biological Sciences, Kangwon National University, Chuncheon, Republic of Korea; [2]Korea Basic Science Institute, Chuncheon Center, Chuncheon, Republic of Korea; [3]Department of New Drug Discovery and Development, Chungnam National University, Daejeon, Republic of Korea; [4]Department of Biochemistry, Yonsei University, Seoul, Republic of Korea; [5]Department of Neurobiology, Kangwon National University, Chuncheon, Republic of Korea and [6]Department of Molecular and Cellular Biochemistry, Kangwon National University, Chuncheon, Republic of Korea
[7]These authors contributed equally to this work.
Correspondence: Professor S Ryoo, Department of Biological Sciences, Kangwon National University, Kangwondae-gil 1, Chuncheon, Kangwon-do 24341, Republic of Korea.
E-mail: ryoosw08@kangwon.ac.kr
Received 16 April 2017; revised 17 July 2017; accepted 23 July 2017

distribution and subcellular localization patterns but share ~60% sequence homology. Arginase hydrolyzes L-arginine to L-ornithine and urea, and L-ornithine plays an important role in the synthesis of polyamine, putrescine, spermidine and spermine.[6] Arginase I is a cytosolic enzyme that is abundantly expressed in the liver and participates in the urea cycle. Arginase II is a mitochondrial protein predominantly expressed in kidney,[7,8] and its activity is enhanced after its subcellular redistribution via activation of the RhoA/Rho kinase pathway.[9] Interestingly, arginase II overexpression induced vascular smooth muscle cell proliferation,[10] caused mitochondrial dysfunction through increased production of mitochondrial reactive oxygen species (ROS),[11] attenuated mitochondrial membrane potential (MMP) and promoted atherogenesis in mouse models.[12] Conversely, arginase II deficiency decreased proinflammatory cytokine levels and resulted in the accumulation of fewer monocytes in the plaque.[11] Arginase inhibition in ApoE$^{-/-}$ mice reduced the area of plaque lesions in the aorta.[13]

However, the arginase isoforms that are dominantly expressed in hAoSMCs are unclear, and the effect of arginase inhibition on inflammation in early atherogenic conditions, such as hyperlipidemia, remains uncharacterized. Furthermore, the effect of arginase activity on mitochondrial function has also not been demonstrated. Therefore, we examined the arginase isoforms expressed in hAoSMCs, tested the mechanism underlying the association between arginase activity and MMP and evaluated whether arginase inhibition attenuated IL-8 production in nLDL-stimulated vascular smooth muscle cells.

MATERIALS AND METHODS

Materials

2(*S*)-Amino-6-boronohexanoic acid (ABH) and *S*-(2-boronoethyl)-I-cysteine (BEC) were purchased from Calbiochem (La Jolla, CA, USA). PCR primers and PCR premix were purchased from Bioneer (Daejeon, South Korea). Anti-sera against arginase I and arginase II were obtained from Santa Cruz Biotechnology (Santa Cruz, CA, USA). β-Tubulin antiserum was obtained from BD Biosciences (San Jose, CA, USA), and the phospho-specific p38 MAPK antibody was purchased from Cell Signaling Technology (Beverly, MA, USA). All other reagents were purchased from Sigma (St Louis, MO, USA) unless otherwise stated.

Cell culture

hAoSMCs (explanted from a 20-year-old male) were purchased from Lonza (Lot No. 7F4322, Allendale, NJ, USA) and cultured in the SmGM-2 Bullet kit in 5% CO_2 at 37 °C. The growth medium was removed and replaced with Dulbecco's modified Eagle's medium containing 0.1% fetal bovine serum (Thermo Fisher Scientific, Waltham, MA, USA) for 24 h before experiments.

Reverse transcription–PCR analysis

Total RNAs were isolated with TRIzol reagent according to the supplier's protocol (Thermo Fisher Scientific), and complementary DNA was synthesized by AMV reverse transcriptase (Invitrogen, Carlsbad, CA, USA). PCR amplification was performed with specific primer sets for human arginase I (forward, 5′-GGCAAGGTG GCAGAAGTCA-3′; reverse, 5′-TGGTTGTCAGTGGAGTGGTTG-3′; product, 163 bp) and arginase II (forward, 5′-CTATCAGCACTGGA TCTTGTTG-3′; reverse, 5′-GGGAGTAGGAAGTTGGTCATAG-3′; product, 156 bp). GAPDH (forward, 5′-ACCACAGTCCATGCCAT CAC-3′; reverse, 5′-TCCACCACCCTGTTGCTGTA-3′; product 476 bp) was amplified as a control.

Arginase activity measurement

Arginase activity was measured by quantifying the amount of urea generated from L-arginine as previously described.[13]

Isolation of nLDL and culture of mASMCs

The nLDL (density 1.019–1.063 g ml^{-1}) was prepared from the plasma of normocholesterolemic subjects by differential ultracentrifugation as previously described.[3] Isolated nLDL did not exhibit oxidative modification within 3 weeks compared with the oxidation of commercial nLDL and oxidized LDL from Intracel (Frederick, MD, USA) as determined by the thiobarbituric-reactive substance assay using malondialdehyde as a standard. ApoE$^{-/-}$ mice (Daehan Biolink, Chungbuk, Korea) were fed a high-cholesterol diet (HCD, D12108C, Research Diet, New Brunswick, NJ, USA) for 8 weeks. Mouse aortic smooth muscle cells (mASMCs) were isolated from the thoracic and upper parts of the abdominal aorta from 10- to 12-week-old male C57BL/6 and arginase II-null (ArgII$^{-/-}$) mice as previously described[14] with minor modifications. Briefly, the stripped aorta was prepared from the anesthetized mouse and cut into 2 mm pieces that were treated with type II collagenase (1 mg ml^{-1}, Invitrogen) for 1 h to remove the endothelial cells and then washed with culture media. The de-endothelialized aortic pieces were incubated with culture medium on a gelatin (0.1%)-coated culture dish for ~10 days. The purity of the mASMC cultures was >95% as confirmed by immunocytochemical staining for α-smooth muscle actin. Passages 2–4 of the mASMCs were used in these experiments. The cells were cultured in Dulbecco's modified Eagle's medium supplemented with 10% fetal bovine serum, 0.5× smooth muscle growth supplement (Cascade Biologics, Portland, OR, USA), 100 U ml^{-1} penicillin, 100 μg ml^{-1} streptomycin, 8 mM HEPES and 2 mM glutamine at 37 °C in a humidified 5% CO_2 incubator.

Arginase II immunostaining

To stain mitochondria, cells cultured on fibronectin (Invitrogen)-coated slides were incubated for 30 min with 25 nM MitoTracker-Red CMXRos (Molecular Probes, Eugene, OR, USA). Cells were fixed and permeabilized with 3% paraformaldehyde and 0.5% Triton X-100 in phosphate-buffered saline, rinsed with phosphate-buffered saline and incubated with polyclonal antibody against arginase II and with Cy5-conjugated anti-rabbit lgG antibody. Images were acquired using epifluorescence microscopy (BX51, Olympus, Shinjuku, Tokyo, Japan) with 579/633 nm excitation and 599/647 nm emission (MitoTracker-Red/ArgII) using a 60× objective. Epifluorescence images were collected using MetaMorph software (Molecular Devices, Downingtown, PA, USA) and an internally cooled iXon^{EM}+860, EMCCD camera (Andor, South Windsor, CT, USA).

Microscopic estimation of MMP using the fluorescence probe TMRE

Starved cells were labeled with a fluorescent probe to tetramethylrhodamine ethyl ester (TMRE; 100 nmol l^{-1}, 37 °C, 30 min) and stimulated with nLDL (100 μg ml^{-1}) in the presence or absence of inhibitors. Images (548 nm excitation and 588 nm emission) were acquired using an up-light Olympus epifluorescence microscope

(BX51, 40× objective) equipped with an internally cooled Clara EMCCD camera[13] and collected using MetaMorph software. The measured fluorescence values were normalized based on cell numbers in the image.

Mitochondria fractionation and western blot analysis

Treated cells were washed twice with phosphate-buffered saline, scraped and centrifuged at 600 *g* for 5 min. The pellet was resuspended in 1 ml of cold mitochondrial isolation buffer containing 0.3 M sucrose, 1 mM EGTA, 5 mM KH_2PO_4 and 0.1% bovine serum albumin (pH 7.4) and then homogenized. Disrupted cells were centrifuged at 2600 *g* for 5 min, and the supernatant was further centrifuged at 15 000 *g* for 10 min at 4 °C to obtain the crude mitochondrial and cytosolic fractions. The resulting supernatant was centrifuged at 100 000 *g* for 1 h to separate the microsomal fraction. The cytosolic and mitochondrial fractions were mixed with 2× SDS sample buffer containing 125 mM Tris (pH 6.8), 4% SDS and 20% glycerol and then sonicated for 5 s. Each sample was resolved on 10% SDS–polyacrylamide gel electrophoresis, transferred to a polyvinylidene difluoride membrane (Amersham Biosciences, Buckinghamshire, UK), analyzed with antibodies according to the supplier's protocol and visualized using peroxidase and an enhanced chemiluminescence system (Intron, seongnam, Gyeonggi, South Korea).

Measurement of mitochondrial Ca^{2+} and ROS in living cells

The cells were seeded on a glass bottom fluoro-dish coated with 0.1% gelatin and cultured in growth and starvation media for 1 day each. Rhod-2 AM (5 μM) was used for Ca^{2+} measurements, and MitoSox-Red (100 μM; Molecular Probes) was used for mitochondrial superoxide measurements. Cells were exposed to dyes in a 37 °C CO_2 incubator for 30 min. Fluorescent images were acquired using a LSM780 NLO confocal microscope (Carl Zeiss, Oberkochen, Germany) using laser light at the following excitation/emission wavelengths: Mitotracker-Green, 490/552 nm; Rhod-2 AM, 516/581 nm; and MitoSox-Red, 510/580 nm. HEPES-buffered Hanks' balanced salt solution was used as the imaging buffer.[15] To confirm the relationship between the fluorescent intensity and $[Ca^{2+}]$m, caffeine was used as a positive control to induce mitochondrial Ca^{2+} uptake.[16] All acquired LSM raw data obtained from imaging were processed using ZEN 2011 software (Carl Zeiss).

Polyamine analysis

Intracellular concentrations of L-arginine and the polyamines spermine, spermidine and putrescine were determined using high-performance liquid chromatography with pre-column derivatization of *o*-phthalaldehyde (OPA). Experiments were performed using previously published methods[17] with some modifications. Briefly, L-arginine (100 μM) and polyamine (30 μM/each) were added to cell lysate (0.1 mM) as an internal standard. Samples were extracted using solid-phase extraction cartridges (CBA Bond elute, Varian, Yverdon, Switzerland). The recovery rate was 87.5 ± 3.9% for L-arginine. Eluates were dried over nitrogen and resuspended in double-distilled water. A computer-controlled Waters chromatography system (M600E) with

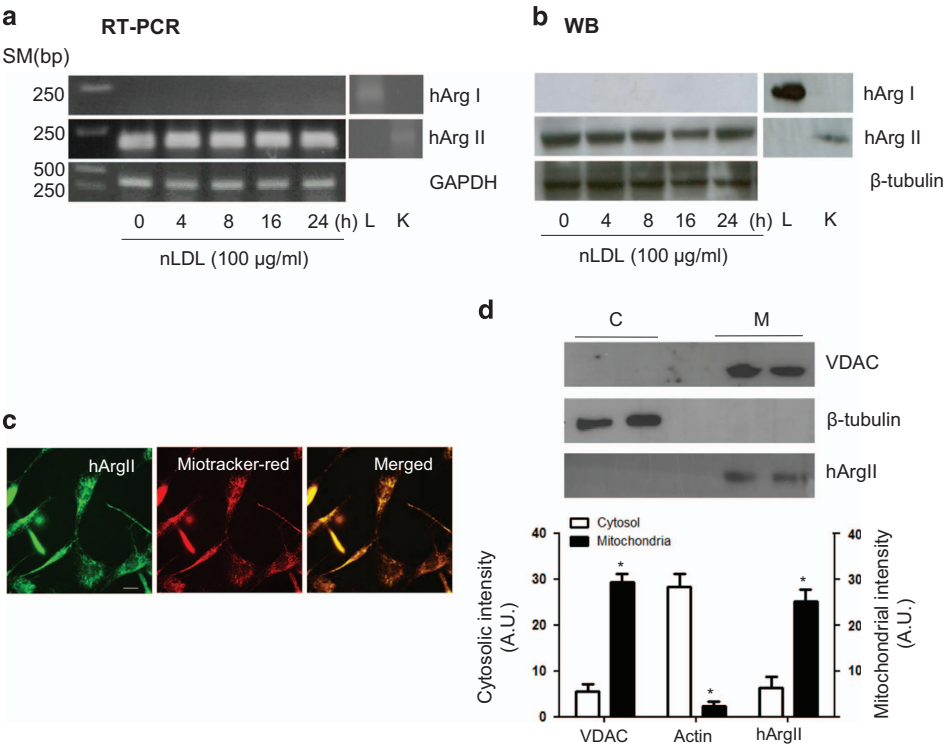

Figure 1 The arginase II isoform is dominantly expressed and targeted to mitochondria in human aortic smooth muscle cells. (**a**) Reverse transcription–PCR (RT-PCR) was performed with isoform-specific primers for arginase I and II after native low-density lipoprotein (nLDL) stimulation at different time intervals. (**b**) Western blotting analysis was performed with specific anti-sera against arginase I and II in cell lysates that were either treated with nLDL or left untreated. L, liver lysate for arginase I, K, kidney lysate for arginase II. (**c**) Cells were stained with the mitochondrial-specific dye MitoTracker-Red and costained with anti-arginase II antibody (green). The scale bar indicates 50 μm. (**d**) The cell lysates were fractionated into cytosolic and mitochondrial fractions, and voltage-dependent anion channel (VDAC) and β-tubulin were used as mitochondrial and cytosolic marker proteins, respectively. Arginase II was identified in the mitochondrial fraction (M) but not in the cytosolic fraction (**c**) in human aortic smooth muscle cells (hAoSMCs; $n=3$) $^*P<0.01$.

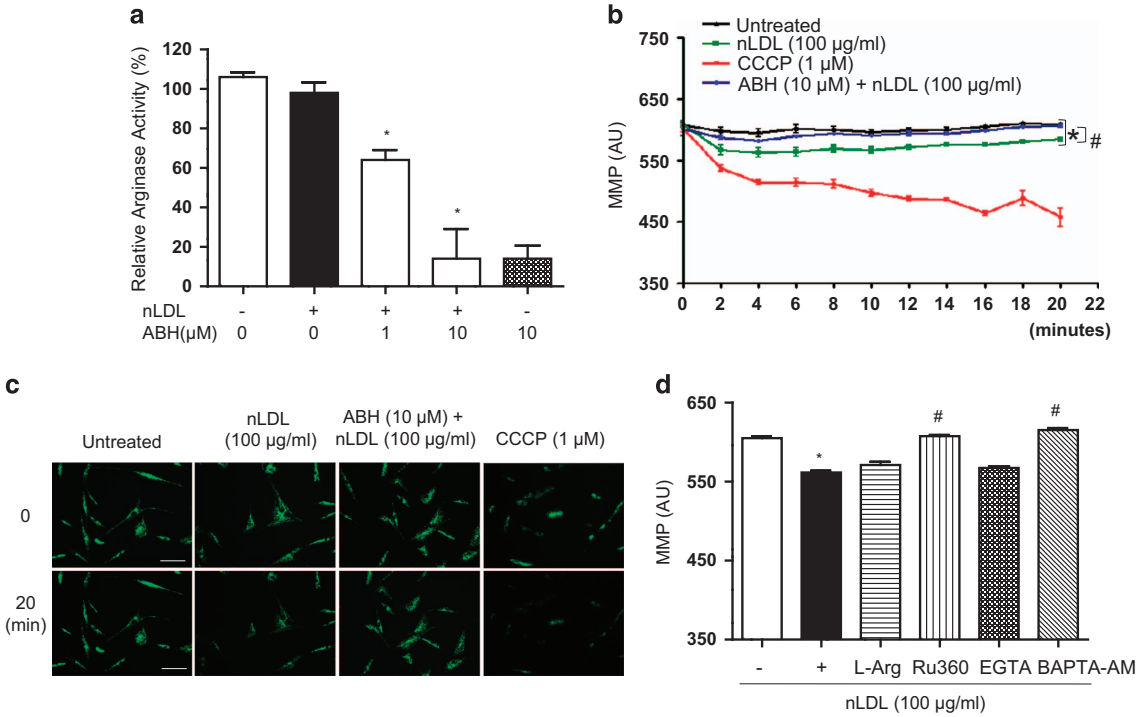

Figure 2 Arginase inhibition restored impaired mitochondrial membrane potential upon native low-density lipoprotein (nLDL) stimulation. (**a**) Arginase activity was measured following nLDL stimulation for 8 h in the presence or absence of the arginase inhibitor 2(*S*)-Amino-6-boronohexanoic acid (ABH). *Vs nLDL alone, $P<0.01$; $n=4$. (**b**) The mean tetramethylrhodamine ethyl ester (TMRE) fluorescence intensity from 20 cells randomly selected over the time course is presented for each group. Similar results were obtained in four independent experiments. Carbonylcyanide-3-chlorophenylhydrazone (CCCP) was used as a control. *Untreated vs nLDL, $P<0.01$; #nLDL vs ABH+nLDL, $P<0.01$. (**c**) Representative images of TMRE fluorescence in each group at 0 and 20 min. The scale bar indicates 200 μm. (**d**) Average values of TMRE fluorescence were acquired 20 min after treatment with nLDL and after preincubation with L-arginine (L-Arg; 10 mM), ruthenium 360 (Ru360; 10 μM), EGTA (50 μM) and BAPTA-AM (10 μM). *Vs nLDL, $P<0.01$; #vs nLDL, $P<0.01$.

an automatic injector (M7725i, Waters, Milford, MA, USA) and fluorescence detector (FP-1520, Jasco, Easton, MD, USA) was used for high-performance liquid chromatography analysis. Samples were incubated for 1 min with OPA reagent (5.4 mg ml^{-1} OPA in borate buffer, pH 8.4, containing 0.4% 2-mercaptoethanol) before automatic injection into the high-performance liquid chromatography machine. The OPA derivative of L-arginine was separated on a 150 × 4.6 mm, 5 μm Zorbax Eclipse (Agilent Technologies, Santa Clara, CA, USA) XDB-C18 column with the fluorescence detector set to an excitation wavelength of 340 nm and an emission wavelength of 450 nm. Samples were eluted from the column with a 70:30 ratio of 0.96% citric acid/methanol pH 6.8 at a flow rate of 1.5 ml min^{-1}.

ELISA for IL-8

The amount of IL-8 released into the medium was measured using a human IL-8 enzyme-linked immunosorbent assay (ELISA) kit II (Opt-EIA, BD Biosciences, San Jose, CA, USA) and mouse KC (IL-8 analog) ELISA kit (Creative Diagnostics, Shirley, NY, USA) according to the manufacturers' instructions. All experiments were conducted in triplicate.[3]

Statistical analysis

All data are presented as mean ± s.d., and unpaired Student's *t*-test was used to assess the significance of differences between the two groups. A value of $P<0.05$ was accepted as significant.

RESULTS

Arginase II is abundantly expressed in mitochondria in human aortic smooth muscle cells

Because arginase II is present predominantly in the mitochondria of human aortic endothelial cells,[18] we determined which isoform was expressed in hAoSMCs. As demonstrated in Figure 1a, the expression of arginase II was identified by its reverse transcription–PCR product in both control and nLDL-stimulated hAoSMCs. On the other hand, arginase I expression was not detected in either condition. We next tested the expression of arginase protein isoforms with nLDL stimulation at different time points (Figure 1b). Consistent with the reverse transcription–PCR results, the expression of arginase II protein was detected with no changes in protein level during nLDL stimulation, whereas arginase I was not detected. To confirm intracellular targeting, we co-stained hAoSMCs with the mitochondria-specific dye MitoTracker-Red and arginase II-specific antiserum (green). Arginase II appears to be localized in the mitochondria, as demonstrated in the merged image depicting both arginase II and MitoTracker-Red (Figure 1c). As demonstrated in the fractionation experiment in Figure 1d, arginase II is predominantly found in the mitochondrial fraction.

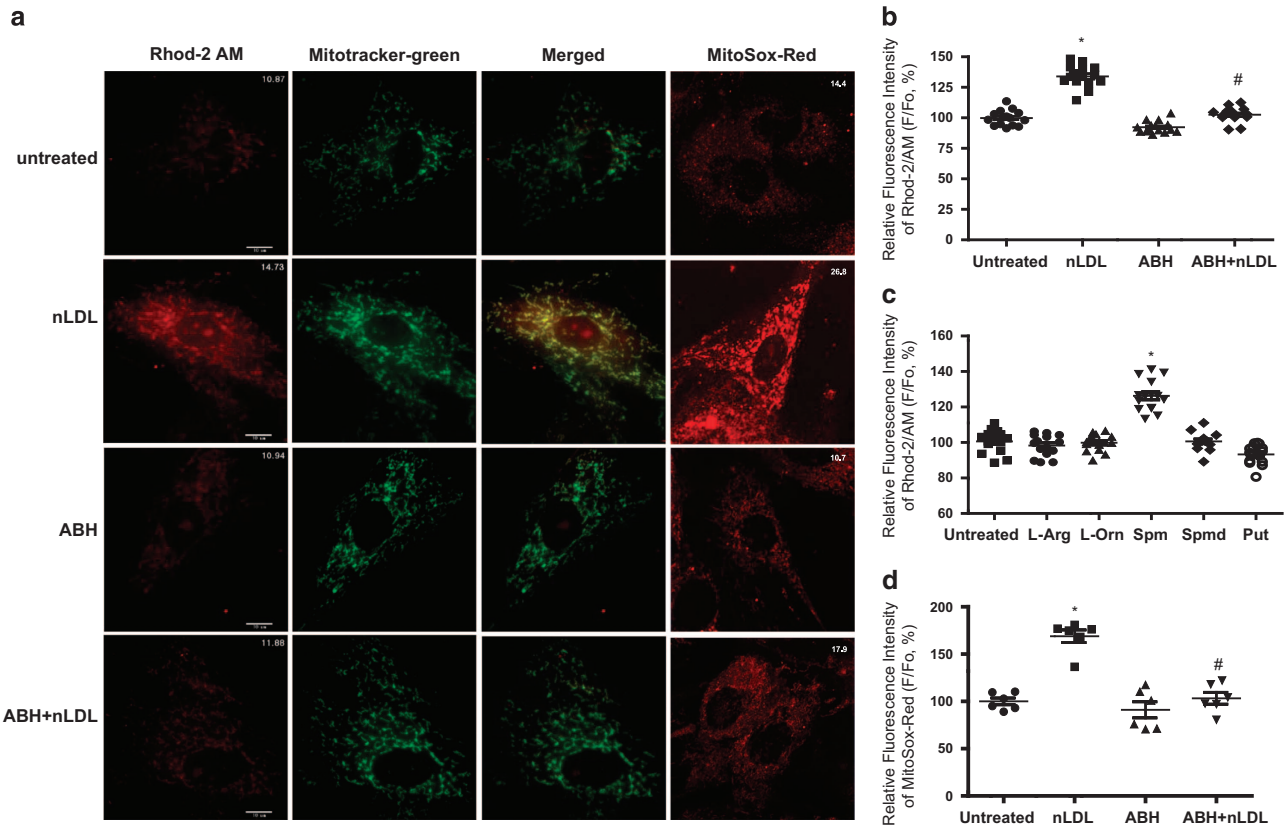

Figure 3 Arginase inhibition prevented mitochondrial Ca^{2+} uptake in native low-density lipoprotein (nLDL)-stimulated human aortic smooth muscle cells (hAoSMCs). Fluorescence intensities of Rhod-2 AM and MitoSox-Red were measured after nLDL stimulation for 30 min. A representative image is presented in (**a**), and the fluorescence intensities of Rhod-2/AM (**b**) and MitoSox-Red (**d**) from three independent experiments are presented as bar graphs. At least five images were obtained for each experiment. *Vs nLDL, $P<0.05$; #vs nLDL, $P<0.05$. Scale bar is 10 μm. (**c**) Starved cells were incubated with L-arginine (L-Arg), L-ornithine (L-Orn), spermine (Spm), spermidine (Spd) and putrescine (Put) at 100 μM for 3 h, and the change in fluorescence intensity in each image was measured. *Vs untreated, $P<0.05$.

Protective effect of arginase inhibition in nLDL-dependent loss of MMP

We next sought to determine arginase activity in nLDL-stimulated hAoSMCs. Arginase activity was not affected by nLDL stimulation (Figure 2a, $n=6$, not significant (NS)). However, the arginase inhibitor ABH inhibited the activity in a dose-dependent manner (*vs nLDL alone, 14.1 ± 26.2 (10 μM) vs $106.7\pm4.3\%$). Given that dyslipidemia induces mitochondrial damage and dysfunction,[19] we next assessed whether nLDL treatment affects the MMP. Starved cells were preincubated with TMRE, and the change in fluorescence intensity was recorded over 20 min. As demonstrated in Figure 2b, the intensity of TMRE fluorescence decreased upon nLDL treatment from 609.3 ± 6.1 to 580.6 ± 13.8 (arbitrary unit (AU)) and persisted for 20 min. Fluorescence was restored to untreated control levels by preincubation with the arginase inhibitor ABH (**nLDL vs ABH+nLDL, 580.6 ± 13.8 vs 606.1 ± 11.1 AU). The uncoupling agent carbonylcyanide-3-chlorophenylhydrazone (CCCP) was used as a control for the loss of MMP (456.9 ± 56.1 AU at 20 min). Representative images are presented in Figure 2c. The restoration of MMP by arginase inhibition was analyzed using TMRE fluorescence and fluorescence-activated cell sorting (FACSAria, BD, Biosciences, San Jose, CA, USA). The decrease in TMRE fluorescence upon nLDL stimulation (100 to 89.1 ± 2.5 AU, $P<0.01$) was restored upon ABH preincubation (nLDL vs ABH+nLDL, 89.1 ± 2.5 vs 97.0 ± 1.4 AU, $P<0.01$, $n=7$). These data analyzed with WinMDI software were consistent with the microscopic measurements. We next examined the effects of L-arginine, BAPTA-AM and ruthenium 360 (Ru360) on the nLDL-induced MMP change (Figure 2d). Interestingly, preincubation of L-Arg did not inhibit the nLDL-dependent decrease in MMP (L-Arg+nLDL vs nLDL, 571.0 ± 14.3 vs 561.6 ± 8.3 AU, NS). However, Ru360, a mitochondrial Ca^{2+} ion channel blocker, blocked the loss of MMP by nLDL (Ru360 +nLDL vs nLDL, 607.5 ± 15.4 vs 561.6 ± 8.3 AU, $P<0.01$). Consistent with the above data, the intracellular Ca^{2+} chelator BAPTA-AM significantly prevented MMP loss in nLDL-treated hAoSMCs (BAPTA-AM+nLDL vs nLDL, 615.3 ± 9.2 vs 561.6 ± 8.3 AU, $P<0.01$). However, EGTA, an extracellular Ca^{2+} chelator, had no effect on MMP loss.

Arginase II activity regulates mitochondrial Ca^{2+} uptake

The above data suggest that intracellular Ca^{2+} may be involved in the maintenance of MMP. Therefore, we next used confocal microscopy with the mitochondrial Ca^{2+}-specific fluorescent

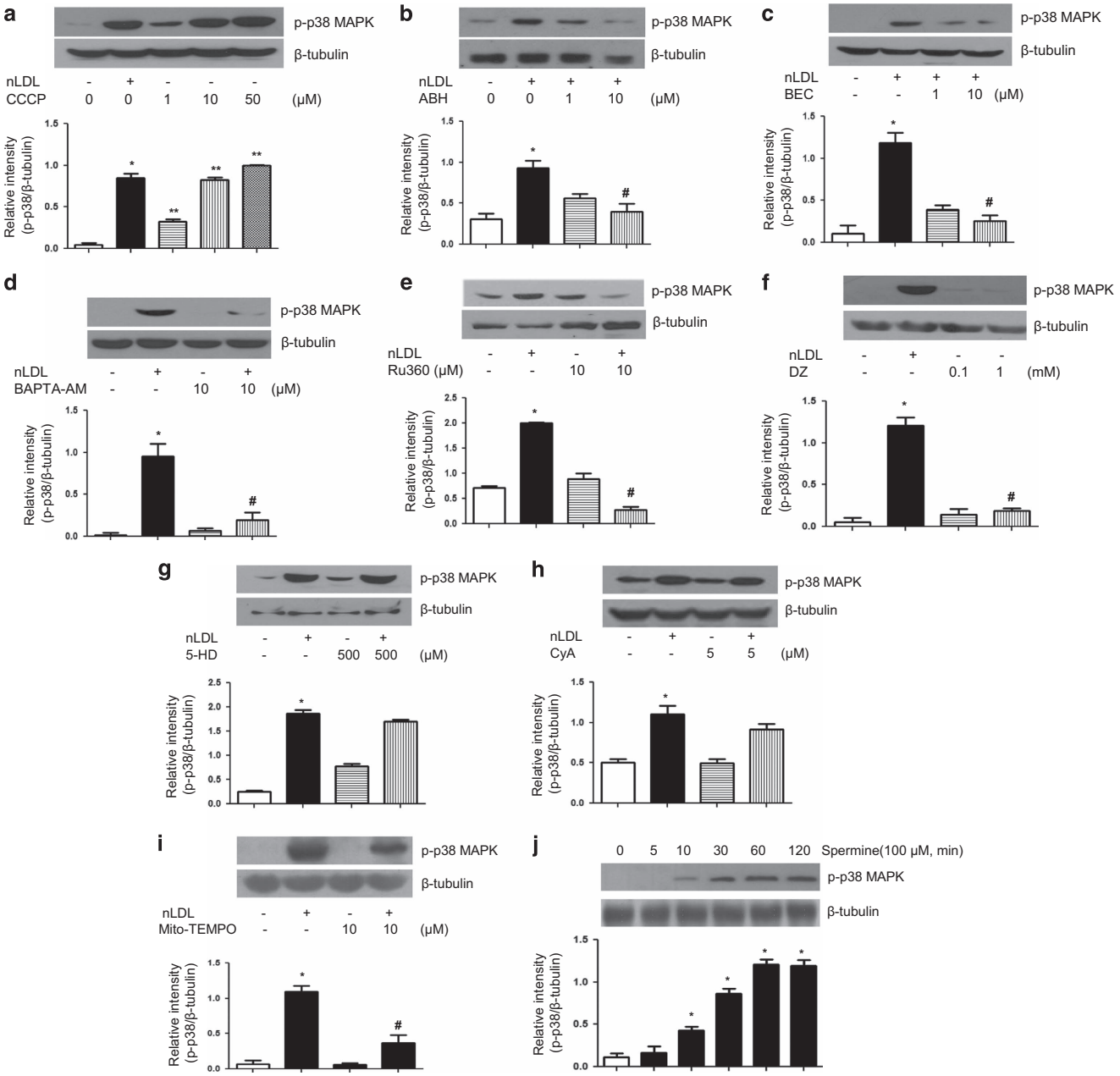

Figure 4 Loss of mitochondrial membrane potential (MMP) was associated with p38 mitogen-activated protein kinase (MAPK) phosphorylation in native low-density lipoprotein (nLDL)-stimulated human aortic smooth muscle cells (hAoSMCs). (**a**) p38 MAPK activation was examined after nLDL treatment (100 μg ml^{-1}) for 5 min and carbonylcyanide-3-chlorophenylhydrazone (CCCP) incubation (1, 10 and 50 μM) for 30 min using western blotting analysis. Preincubation with the arginase inhibitors (**b**) 2(*S*)-Amino-6-boronohexanoic acid (ABH) and (**c**) *S*-(2-boronoethyl)-l-cysteine (BEC) attenuated p38 MAPK activation in a dose-dependent manner. (**d**) BAPTA-AM and (**e**) ruthenium 360 (Ru360 inhibited p38 MAPK activation. (**f**) Diazoxid (DZ), (**g**) 5-hydroxydecanoic acid (5-HD) and (**h**) cyclosporin A (CyA) did not affect nLDL-induced p38 MAPK activation. (**i**) The mitochondrial reactive oxygen species (ROS) scavenger Mito-TEMPO abolished nLDL-induced phosphorylation of p38 MAPK. (**j**) Spermine treatment induced p38 MAPK phosphorylation in a time-dependent manner; $n=3$. * vs. untreated control, $P<0.05$; ** vs. untreated control, $P<0.01$; # vs. nLDL only, $P<0.01$

dye Rhod-2 AM to assess whether arginase inhibition regulates mitochondrial Ca^{2+} levels. As shown in Figures 3a and b, nLDL stimulation induced Ca^{2+} uptake into mitochondria (*untreated vs nLDL, 100.0 ± 6.2 vs $133.9\pm9.0\%$, $P<0.05$) that was completely prevented with the preincubation of arginase inhibitor (#nLDL vs nLDL+ABH, 133.9 ± 9.0 vs $102.5\pm6.0\%$, $P<0.05$). To clearly demonstrate that the fluorescence arose from mitochondria, we simultaneously stained the cells with Mitotracker-Green. As shown in the merged image, the fluorescence of Rhod-2 AM overlapped completely with that of Mitotracker-Green. Furthermore, we confirmed the generation of mitochondrial superoxide using

MitoSox-Red (Figures 3a and d). nLDL stimulation induced the generation of ROS in mitochondria, and this induction was not observed when arginase was inhibited (*untreated vs nLDL, 100.0 ± 8.9 vs $168.9 \pm 16.3\%$, $P<0.05$; #nLDL vs nLDL+ABH, 168.9 ± 16.3 vs $103.3 \pm 15.2\%$, $P<0.05$). Next, we investigated which molecule related to arginase activity is responsible for Ca^{2+} uptake into mitochondria. Interestingly, only the polyamine spermine induced an increase in mitochondrial Ca^{2+} levels (Figure 3c, untreated vs spermine, 100.0 ± 6.3 vs $126.2 \pm 8.6\%$, $P<0.05$). These results suggest that the prevention of Ca^{2+} uptake into mitochondria by arginase inhibition is dependent on a spermine-associated mechanism.

Altered MMP results in p38 MAPK activation and IL-8 production in nLDL-stimulated hAoSMCs

We next sought to determine whether the loss of MMP upon nLDL stimulation was associated with p38 MAPK activation. The uncoupling agent CCCP induced p38 MAPK phosphorylation in a dose-dependent manner (Figure 4a). Interestingly, pretreatment with arginase inhibitors (Figures 4b and c) prevented the phosphorylation of p38 MAPK by nLDL stimulation in a dose-dependent manner. BAPTA-AM and Ru360 also inhibited p38 MAPK phosphorylation (Figures 4d and e). However, other inhibitors of mitoK_{ATP} (5-hydroxydecanoic acid) and the mitochondrial permeability transition pore (cyclosporine A) and an activator of mitoK_{ATP} (diazoxid) did not have any effect on p38 MAPK activation (Figures 4f–h). Interestingly, the mitochondrial ROS scavenger Mito-TEMPO prevented nLDL-dependent p38 MAPK activation (Figure 4i), and spermine treatment induced p38 MAPK phosphorylation in a time-dependent manner (Figure 4j).

As shown in Figure 5, arginase inhibitors significantly attenuated IL-8 production in nLDL-stimulated hAoSMCs (##vs nLDL, 10.9 ± 0.1 vs 13.4 ± 0.6 ng ml^{-1}, $P<0.01$); however, the p38 MAPK inhibitor SB203580 completely inhibited IL-8 production (#vs nLDL, 3.1 ± 0.1 vs 13.4 ± 0.6 ng ml^{-1}, $P<0.01$). Whereas 5-hydroxydecanoic acid did not have any effect on IL-8 production (5-hydroxydecanoic acid vs nLDL, NS), BAPTA and Ru360 completely abolished IL-8 production (**vs nLDL, 4.9 ± 0.1 vs 13.4 ± 0.6 ng ml^{-1}, $P<0.01$; ***vs nLDL, 5.1 ± 0.2 vs 13.4 ± 0.6 ng ml^{-1}, $P<0.01$). These data are consistent with previous observations that arginase II deficiency decreased the amounts of proinflammatory cytokines and resulted in monocyte accumulation into the plaque area[11] and that the arginase inhibitor reduced plaque formation in ApoE$^{-/-}$ mice fed a HCD.[13]

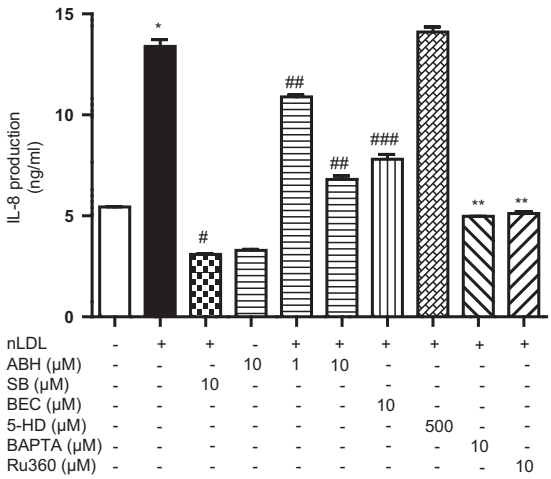

Figure 5 Arginase II inhibition attenuated interleukin-8 (IL-8) production. Native low-density lipoprotein (nLDL)-stimulated IL-8 production (*$P<0.01$) was completely blocked by incubation with a p38 mitogen-activated protein kinase (MAPK) inhibitor (SB203580 (SB), 10 μM, #$P<0.01$). 2(*S*)-Amino-6-boronohexanoic acid (ABH) and *S*-(2-boronoethyl)-l-cysteine (BEC) attenuated IL-8 production in a dose-dependent manner (###$P<0.01$), whereas 5-hydroxydecanoic acid (5-HD) had no effect. Preincubation with BAPTA-AM (10 μM) and ruthenium 360 (Ru360; 10 μM) prevented IL-8 production (**$P<0.01$). Data are derived from four independent experiments.

As shown in Figure 5, arginase inhibitors significantly attenuated IL-8 production in nLDL-stimulated hAoSMCs (##vs nLDL, 10.9 ± 0.1 vs 13.4 ± 0.6 ng ml^{-1}, $P<0.01$); however, the p38 MAPK inhibitor SB203580 completely inhibited IL-8 production (#vs nLDL, 3.1 ± 0.1 vs 13.4 ± 0.6 ng ml^{-1}, $P<0.01$). Whereas 5-hydroxydecanoic acid did not have any effect on IL-8 production (5-hydroxydecanoic acid vs nLDL, NS), BAPTA and Ru360 completely abolished IL-8 production (**vs nLDL, 4.9 ± 0.1 vs 13.4 ± 0.6 ng ml^{-1}, $P<0.01$; ***vs nLDL, 5.1 ± 0.2 vs 13.4 ± 0.6 ng ml^{-1}, $P<0.01$). These data are consistent with previous observations that arginase II deficiency decreased the amounts of proinflammatory cytokines and resulted in monocyte accumulation into the plaque area[11] and that the arginase inhibitor reduced plaque formation in ApoE$^{-/-}$ mice fed a HCD.[13]

p38 MAPK-dependent IL-8 production by nLDL stimulation is reduced in mASMCs from ArgII$^{-/-}$ mice

We first measured MMP changes in isolated mASMCs from wild-type (WT) and ArgII$^{-/-}$ mice. nLDL stimulation induced MMP loss in mASMCs from WT mice (*untreated vs nLDL, 100 ± 6.4 vs $81.5 \pm 4.8\%$, $P<0.05$) but not in cells from ArgII$^{-/-}$ mice (untreated vs nLDL, 121.4 ± 6.1 vs $118.6 \pm 4.5\%$, NS). Furthermore, the MMP in untreated cells was maintained at higher values in ArgII$^{-/-}$ mice compared with WT mice (**WT vs ArgII$^{-/-}$, 100 ± 6.4 vs 121.4 ± 6.1, $P<0.01$; Figure 6a). Measurement of mitochondrial Ca^{2+} using Rhod-2 AM revealed that nLDL treatment induced a marked increase in mitochondrial Ca^{2+} in WT cells (*untreated vs nLDL, 100 ± 6.3 vs$122 \pm 7.5\%$, $P<0.05$). However, in mASMCs from ArgII$^{-/-}$ mice, mitochondrial Ca^{2+} was not altered by nLDL stimulation (untreated vs nLDL, 82.2 ± 5.5 vs $86.0 \pm 7.1\%$, NS) and remained at a lower level compared with in WT (**WT vs ArgII$^{-/-}$, 100 ± 6.3 vs 82.2 ± 5.5, $P<0.05$; Figure 6b). Next, we assessed whether the difference in MMP is associated with p38 MAPK activation. The maintenance of high MMP in ArgII$^{-/-}$ caused a decrease in p38 MAPK activation upon nLDL stimulation (Figure 6c, *WT vs ArgII$^{-/-}$, relative intensity, 89.6 ± 5.8 vs 62.8 ± 4.3 AU, $P<0.01$) that was associated with the production of KC, an IL-8 analog (Figure 6d, *WT vs ArgII$^{-/-}$, 10.3 ± 0.3 vs 5.3 ± 0.3 ng ml^{-1}, $P<0.01$).

Increased arginase activity in ApoE$^{-/-}$ mice fed a HCD increased p38 MAPK phosphorylation, mitochondrial Ca^{2+} and KC production

In isolated mASMCs from ApoE$^{-/-}$ mice fed a HCD, arginase activity (Figure 7a, *WT+normal diet (ND, normal diet) vs ApoE$^{-/-}$+HCD, 100.0 ± 6.9 vs $126.8 \pm 8.5\%$, $P<0.05$) and spermine levels (Figure 7b, *WT+ND vs ApoE$^{-/-}$+HCD, 100.0 ± 0.8 vs $136.0 \pm 0.8\%$, $P<0.05$) were significantly increased. Consistent with the above results, p38 MAPK phosphorylation increased, but no protein level change was observed for arginase II (Figure 7c). Mitochondrial Ca^{2+} levels (Figure 7d, *WT+ND vs ApoE$^{-/-}$+HCD, 100.0 ± 10.2 vs

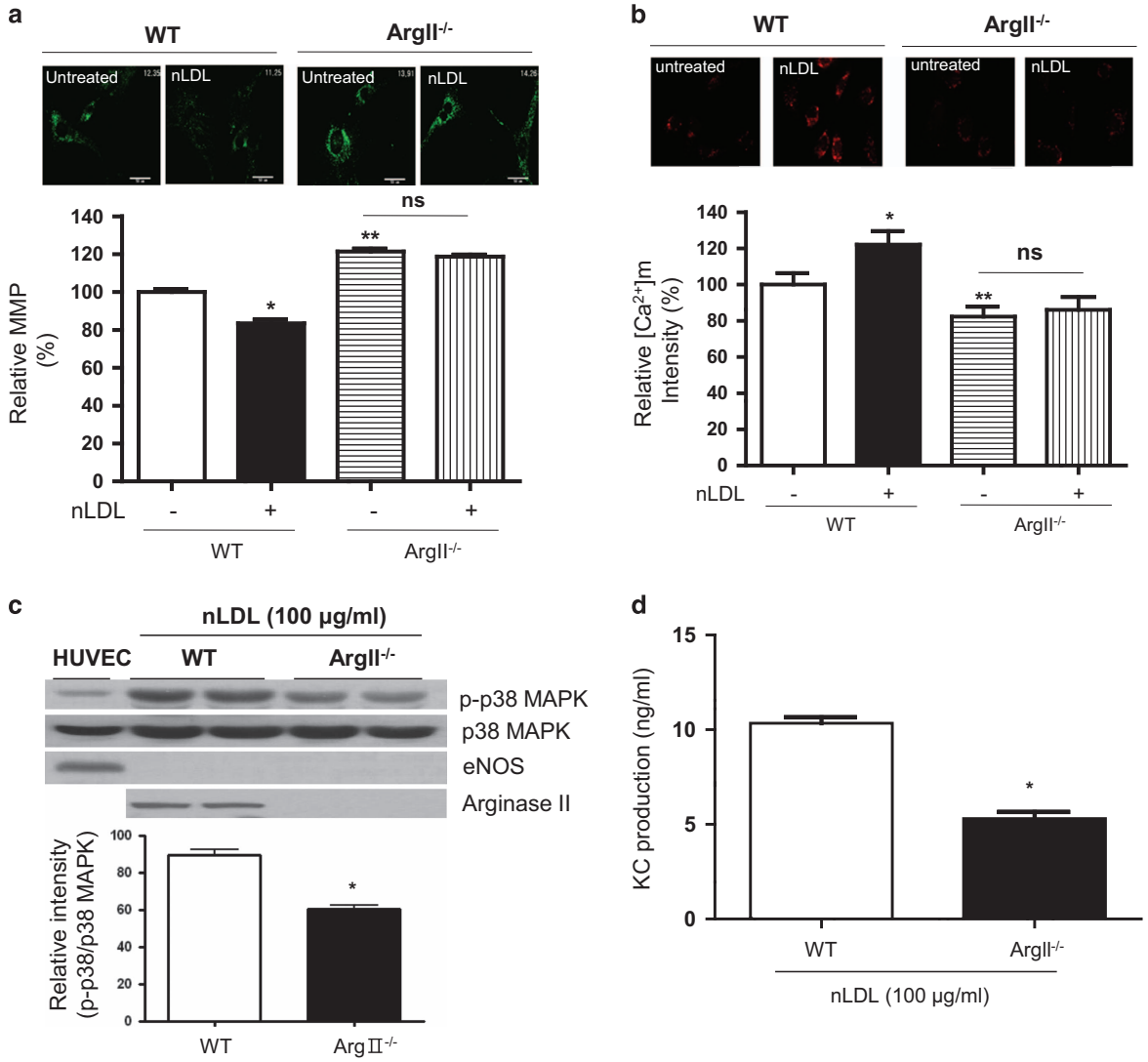

Figure 6 Arginase II gene deficiency inhibited mitochondrial membrane potential (MMP)-dependent p38 mitogen-activated protein kinase (MAPK) activation in native low-density lipoprotein (nLDL)-treated Mouse aortic smooth muscle cells (mASMCs). (**a**) Starved mASMCs isolated from aortas of wild-type (WT) and ArgII$^{-/-}$ mice were stimulated with nLDL (100 μg ml^{-1}, 20 min), and tetramethylrhodamine ethyl ester (TMRE) fluorescent intensity was imaged (up) and displayed as a bar graph (down). *Vs WT+untreated, $P<0.05$; **vs WT+untreated, $P<0.05$. Scale bar is 50 μm. (**b**) Mitochondrial Ca^{2+} was imaged using Rhod-2 AM. *Vs WT+untreated, $P<0.05$; **vs WT+untreated, $P<0.05$. Scale bar is 50 μm. (**c**) The lysates of isolated mASMCs were tested to p38 MAPK activation. *Vs WT, $P<0.01$. (**d**) After nLDL treatment for 24 h, the production of KC (an interleukin-8 (IL-8) analog) was examined using mouse KC ELISA kit. *Vs WT, $P<0.01$.

145.6 ± 12.1%, $P<0.05$) and KC production (Figure 7e, *WT +ND vs ApoE$^{-/-}$+HCD, 4.3 ± 0.1 vs 12.9 ± 0.4 ng ml^{-1}, $P<0.05$) were increased compared with that noted in mASMCs from WT fed a ND.

DISCUSSION

Our results from this study indicated that arginase II was predominantly targeted to mitochondria in hAoSMCs. Arginase II inhibition restored the nLDL-dependent MMP loss that was attributed to inhibition of mitochondrial Ca^{2+} movement. The polyamine spermine enhanced the amount of mitochondrial Ca^{2+}. The change in MMP was associated with p38 MAPK activation and IL-8 production. These results were consistent with our observations in mASMCs isolated from arginase II-null mice.

In the present study, we demonstrated that arginase II is the dominantly expressed isoform in hAoSMCs; however, Wang *et al.*[20] previously demonstrated that arginase I is the dominant isoform in hAoSMCs. Although arginase II expression is developmentally regulated[21] and predominantly noted in human and mouse endothelial cells,[18,22] the expression patterns of isoforms in specific tissues requires further clarification.

Here, we present a novel vasoprotective effect of arginase inhibition that occurs via prevention of MMP loss under hyperlipidemic conditions in hAoSMCs. nLDL incubation

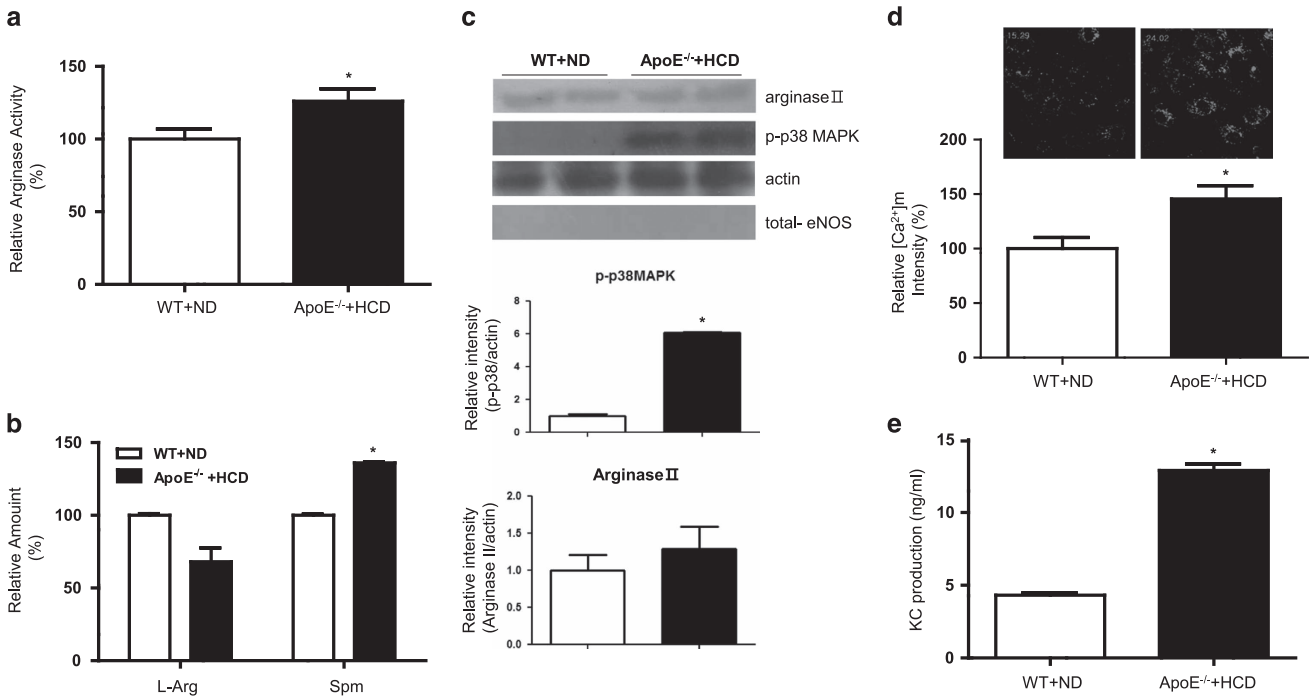

Figure 7 Arginase activity, spermine levels, p38 mitogen-activated protein kinase (MAPK) phosphorylation, mitochondrial Ca^{2+} levels and KC production were increased in $ApoE^{-/-}$ mice fed a high-cholesterol diet (HCD). (**a**) Arginase activity, (**b**) spermine levels and (**c**) p38 MAPK phosphorylation were measured in de-endothelialized aortas of wild-type (WT) mice fed a normal diet (ND) and $ApoE^{-/-}$ mice fed a HCD for 8 weeks. *Vs WT+ND, $P<0.05$. Mitochondrial Ca^{2+} levels in isolated mouse aortic smooth muscle cells (mAoSMCs) were measured with (**d**) Rhod-2 AM, and (**e**) KC production in serum was analyzed using enzyme-linked immunosorbent assay (ELISA). *Vs WT+ND, $P<0.05$.

evoked MMP losses of ~4.7% (microscopic analysis) or 10% (fluorescence-activated cell sorting analysis), a relatively small change compared with that observed during H_2O_2 and oxidized LDL stimulation. This result may be attributed to differences in the effects of these treatments on cellular processes, such as proliferation and apoptosis. Indeed, H_2O_2 and oxidized LDL induced cellular apoptosis with a significant decrease of MMP in macrophages[23] and cardiac myocytes.[24] Therefore, the difference in MMP loss may play a critical role in the fate of the cell, that is, death and proliferation. In this context, apoptotic signals induce p38 MAPK activation that is associated with altered MMP;[25] however, stress signals, such as high glucose, initially alter the MMP that subsequently induces p38 MAPK activation.[26]

The nLDL-stimulated MMP loss suggested the translocation of a cationic ion into the mitochondrial matrix because a negative MMP (−180 mV) is generally noted.[27] Among the cationic ions, Ca^{2+} in the mitochondrial matrix can enhance the rate of mitochondrial energy production through the activation of dehydrogenases involved in the Krebs cycle[28] and those involved in the activation F_0F_1ATPase[29] and adenine nucleotide translocase[30] in the electron transport chain. Thus, increased Ca^{2+} uptake into the mitochondria in nLDL-stimulated vascular smooth muscle cells appears to be an essential phenomenon because nLDL primarily serves to supply lipids and is then catabolized through mitochondrial β-oxidation to acetyl-CoA that is utilized in energy production (adenosine triphosphate (ATP)). Consistent with these observations, our data demonstrated that nLDL stimulation induced the MMP loss that was recovered by BAPTA-AM (Figures 2b and c). Furthermore, the mitochondrial Ca^{2+} level was high in nLDL-stimulated hAoSMCs (Figures 3a and b). However, arginase inhibition restored nLDL-stimulated MMP loss (Figure 2) that is associated with mitochondrial Ca^{2+} uptake (Figure 3). Among the substrate and products of arginase, only spermine treatment induced an increase in mitochondrial Ca^{2+} level (Figure 3c). Arginase activity plays an important role in the maintenance of the intracellular concentration of spermine (Supplementary Figure 1).[31,32] However, arginase II gene deletion demonstrated that the spermine level was not altered.[33] These reports demonstrate that intracellular levels of spermine play critical roles in the homeostasis of normal cell physiology and that these levels are maintained through metabolic pathways, such as the L-glutamine/glutamate pathway.[34]

In this context, several mitochondrial Ca^{2+} channels are involved in Ca^{2+} uptake into mitochondria.[35] Among these channels, the mitochondrial Ca^{2+} uniporter and rapid mode of uptake are inhibited by Ru360 and activated by spermine.[35] Among putrescine, spermidine and spermine, only spermine induced an increase in mitochondrial Ca^{2+} level. The polyamines putrescine, spermidine and spermine are amino-aliphatic molecules that are almost completely protonated at physiological pH. Therefore, these polyamines interact as

polycations with polyanionic groups on nucleic acids, proteins and membranes. Polyamine binding sites have a distinct flexible structure that can be modified during interactions with these polycations. Previous studies on the binding of polyamines to liver mitochondria identified two specific sites, S_1 and S_2, that exhibit low affinity, high binding capacity, monocoordination and a negligible cooperation effect. The sites are located on the outer membrane and/or on the external surface of the inner membrane.[36] These polyamine binding sites have been characterized. Spermine and spermidine bind to both sites, whereas putrescine exclusively binds to S_2.[36,37] Indeed, the differences in the binding capacity of each of these sites to polyamines may be due to differences in the flexibility and hydration of the polyamines themselves. Spermine is more flexible than spermidine, whereas putrescine is completely rigid. Furthermore, spermine, which has 4 positive charges, is the most hydrated, whereas putrescine, which has 2 positive charges, is the least hydrated.[38] Therefore, the flexible and highly hydrated spermine can bind a rigid and hydrophilic S_1 site. The less flexible spermidine can bind only partially, and the completely rigid putrescine cannot bind. Site S_2 is a flexible and less hydrophilic site and therefore is able to bind spermidine and putrescine. Taken together, spermine binds to the S_1 site and stimulates mitochondrial Ca^{2+} uptake,[37] whereas spermidine was fivefold less effective than spermine. Putrescine was ineffective.[39] Spermine induced mitochondrial Ca^{2+} uptake through the rapid mode of Ca^{2+} uptake (RaM).[40]

In conclusion, we demonstrated that the nLDL-dependent change in MMP through mitochondrial Ca^{2+} uptake is essential for mitochondrial ROS-induced p38 MAPK phosphorylation and IL-8 production and could be blocked by inhibiting arginase II activity.

CONFLICT OF INTEREST

The authors declare no conflict of interest.

ACKNOWLEDGEMENTS

This study was supported by the Basic Science Research Program of the National Research Foundation of Korea funded by the Ministry of Education, Science and Technology (2015R1D1A3A01017911, 2015M3A9B6066968 and 2016M3A9B6903185).

PUBLISHER'S NOTE

1 Sachinidis A, Mengden T, Locher R, Brunner C, Vetter W. Novel cellular activities for low density lipoprotein in vascular smooth muscle cells. *Hypertension* 1990; **15**: 704–711.
2 Locher R, Brandes RP, Vetter W, Barton M. Native LDL induces proliferation of human vascular smooth muscle cells via redox-mediated activation of ERK 1/2 mitogen-activated protein kinases. *Hypertension* 2002; **39**: 645–650.
3 Ryoo SW, Kim DU, Won M, Chung KS, Jang YJ, Oh GT *et al.* Native LDL induces interleukin-8 expression via H_2O_2, p38 Kinase, and activator protein-1 in human aortic smooth muscle cells. *Cardiovasc Res* 2004; **62**: 185–193.
4 Lim HK, Ryoo S. Native low-density lipoprotein-dependent interleukin-8 production through pertussis toxin-sensitive G-protein coupled receptors and hydrogen peroxide generation contributes to migration of human aortic smooth muscle cells. *Yonsei Med J* 2011; **52**: 413–419.
5 Gerszten RE, Garcia-Zepeda EA, Lim YC, Yoshida M, Ding HA, Gimbrone MA *et al.* MCP-1 and IL-8 trigger firm adhesion of monocytes to vascular endothelium under flow conditions. *Nature* 1999; **398**: 718–723.
6 Morris SM, Jr. Arginine metabolism in vascular biology and disease. *Vasc Med* 2005; **10**(Suppl 1): S83–S87.
7 Morris SM, Jr. Arginine metabolism: boundaries of our knowledge. *J Nutr* 2007; **137**: 1602S–1609S.
8 Pernow J, Jung C. Arginase as a potential target in the treatment of cardiovascular disease: reversal of arginine steal? *Cardiovasc Res* 2013; **98**: 334–343.
9 Ryoo S, Bhunia A, Chang F, Shoukas A, Berkowitz DE, Romer LH. OxLDL-dependent activation of arginase II is dependent on the LOX-1 receptor and downstream RhoA signaling. *Atherosclerosis* 2011; **214**: 279–287.
10 Chen B, Calvert AE, Cui H, Nelin LD. Hypoxia promotes human pulmonary artery smooth muscle cell proliferation through induction of arginase. *Am J Physiol Lung Cell Mol Physiol* 2009; **297**: L1151–L1159.
11 Ming XF, Rajapakse AG, Yepuri G, Xiong Y, Carvas JM, Ruffieux J *et al.* Arginase II promotes macrophage inflammatory responses through mitochondrial reactive oxygen species, contributing to insulin resistance and atherogenesis. *J Am Heart Assoc* 2012; **1**: e000992.
12 Xiong Y, Yu Y, Montani JP, Yang Z, Ming XF. Arginase-II induces vascular smooth muscle cell senescence and apoptosis through p66Shc and p53 independently of its l-arginine ureahydrolase activity: implications for atherosclerotic plaque vulnerability. *J Am Heart Assoc* 2013; **2**: e000096.
13 Ryoo S, Gupta G, Benjo A, Lim HK, Camara A, Sikka G *et al.* Endothelial arginase II: a novel target for the treatment of atherosclerosis. *Circ Res* 2008; **102**: 923–932.
14 Wang Y, Lindstedt KA, Kovanen PT. Mast cell granule remnants carry LDL into smooth muscle cells of the synthetic phenotype and induce their conversion into foam cells. *Arterioscler Thromb Vasc Biol* 1995; **15**: 801–810.
15 Palmer AE, Tsien RY. Measuring calcium signaling using genetically targetable fluorescent indicators. *Nat Protoc* 2006; **1**: 1057–1065.
16 Katsuragi T, Sato C, Usune S, Ueno S, Segawa M, Migita K. Caffeine-inducible ATP release is mediated by Ca^{2+}-signal transducing system from the endoplasmic reticulum to mitochondria. *Naunyn Schmiedebergs Arch Pharmacol* 2008; **378**: 93–101.
17 Boger RH, Bode-Boger SM, Mugge A, Kienke S, Brandes R, Dwenger A *et al.* Supplementation of hypercholesterolaemic rabbits with L-arginine reduces the vascular release of superoxide anions and restores NO production. *Atherosclerosis* 1995; **117**: 273–284.
18 Ryoo S, Lemmon CA, Soucy KG, Gupta G, White AR, Nyhan D *et al.* Oxidized low-density lipoprotein-dependent endothelial arginase II activation contributes to impaired nitric oxide signaling. *Circ Res* 2006; **99**: 951–960.
19 Madamanchi NR, Runge MS. Mitochondrial dysfunction in atherosclerosis. *Circ Res* 2007; **100**: 460–473.
20 Wang XP, Chen YG, Qin WD, Zhang W, Wei SJ, Wang J *et al.* Arginase I attenuates inflammatory cytokine secretion induced by lipopolysaccharide in vascular smooth muscle cells. *Arterioscler Thromb Vasc Biol* 2011; **31**: 1853–1860.
21 Belik J, Shehnaz D, Pan J, Grasemann H. Developmental changes in arginase expression and activity in the lung. *Am J Physiol Lung Cell Mol Physiol* 2008; **294**: L498–L504.
22 Lim HK, Ryoo S, Benjo A, Shuleri K, Miriel V, Baraban E *et al.* Mitochondrial arginase II constrains endothelial NOS-3 activity. *Am J Physiol Heart Circ Physiol* 2007; **293**: H3317–H3324.
23 Asmis R, Begley JG. Oxidized LDL promotes peroxide-mediated mitochondrial dysfunction and cell death in human macrophages: a caspase-3-independent pathway. *Circ Res* 2003; **92**: e20–e29.
24 Akao M, O'Rourke B, Teshima Y, Seharaseyon J, Marban E. Mechanistically distinct steps in the mitochondrial death pathway triggered by oxidative stress in cardiac myocytes. *Circ Res* 2003; **92**: 186–194.
25 Farley N, Pedraza-Alva G, Serrano-Gomez D, Nagaleekar V, Aronshtam A, Krahl T *et al.* p38 mitogen-activated protein kinase mediates the Fas-induced mitochondrial death pathway in $CD8^+$ T cells. *Mol Cell Biol* 2006; **26**: 2118–2129.

26 Hou T, Zhang X, Xu J, Jian C, Huang Z, Ye T *et al.* Synergistic triggering of superoxide flashes by mitochondrial Ca^{2+} uniport and basal reactive oxygen species elevation. *J Biol Chem* 2013; **288**: 4602–4612.
27 Bernardi P. Mitochondrial transport of cations: channels, exchangers, and permeability transition. *Physiol Rev* 1999; **79**: 1127–1155.
28 Jouaville LS, Pinton P, Bastianutto C, Rutter GA, Rizzuto R. Regulation of mitochondrial ATP synthesis by calcium: evidence for a long-term metabolic priming. *Proc Natl Acad Sci USA* 1999; **96**: 13807–13812.
29 Territo PR, Mootha VK, French SA, Balaban RS. Ca(2+) activation of heart mitochondrial oxidative phosphorylation: role of the F(0)/F(1)-ATPase. *Am J Physiol Cell Physiol* 2000; **278**: C423–C435.
30 McCormack JG, Halestrap AP, Denton RM. Role of calcium ions in regulation of mammalian intramitochondrial metabolism. *Physiol Rev* 1990; **70**: 391–425.
31 Woo A, Shin W, Cuong TD, Min B, Lee JH, Jeon BH *et al.* Arginase inhibition by piceatannol-3'-O-beta-D-glucopyranoside improves endothelial dysfunction via activation of endothelial nitric oxide synthase in ApoE-null mice fed a high-cholesterol diet. *Int J Mol Med* 2013; **31**: 803–810.
32 Shin WS, Berkowitz DE, Ryoo SW. Increased arginase II activity contributes to endothelial dysfunction through endothelial nitric oxide synthase uncoupling in aged mice. *Exp Mol Med* 2012; **44**: 594–602.
33 Hardbower DM, Asim M, Murray-Stewart T, Casero RA Jr, Verriere T, Lewis ND *et al.* Arginase 2 deletion leads to enhanced M1 macrophage activation and upregulated polyamine metabolism in response to Helicobacter pylori infection. *Amino Acids* 2016; **48**: 2375–2388.
34 Wu G, Flynn NE, Knabe DA. Enhanced intestinal synthesis of polyamines from proline in cortisol-treated piglets. *Am J Physiol Endocrinol Metab* 2000; **279**: E395–E402.
35 Santo-Domingo J, Demaurex N. Calcium uptake mechanisms of mitochondria. *Biochim Biophys Acta* 2010; **1797**: 907–912.
36 Dalla Via L, Di Noto V, Siliprandi D, Toninello A. Spermine binding to liver mitochondria. *Biochim Biophys Acta* 1996; **1284**: 247–252.
37 Dalla Via L, Di Noto V, Toninello A. Binding of spermidine and putrescine to energized liver mitochondria. *Arch Biochem Biophys* 1999; **365**: 231–238.
38 Weiger TM, Langer T, Hermann A. External action of di- and polyamines on maxi calcium-activated potassium channels: an electrophysiological and molecular modeling study. *Biophys J* 1998; **74**: 722–730.
39 Lenzen S, Hickethier R, Panten U. Interactions between spermine and Mg^{2+} on mitochondrial Ca^{2+} transport. *J Biol Chem* 1986; **261**: 16478–16483.
40 Buntinas L, Gunter KK, Sparagna GC, Gunter TE. The rapid mode of calcium uptake into heart mitochondria (RaM): comparison to RaM in liver mitochondria. *Biochim Biophys Acta* 2001; **1504**: 248–261.

Supplementary Information accompanies the paper on Experimental & Molecular Medicine website (http://www.nature.com/emm)